I J C R M
International Journal of Contemporary Research In Multidisciplinary

*Research Article*

# Transient Boundary-Layer Dynamics of An Elastico-Viscous Medium Across a Deformable Sheet Subjected to Chemical Reactivity

**Bikash Koli Saha ***
Independent Researcher, Mathematics, Guwahati, Assam, India

**Corresponding Author:** * Bikash Koli Saha

**DOI:** https://doi.org/10.5281/zenodo.17532511

## Abstract

The transient boundary-layer evolution of an elastico-viscous medium along a persistently deforming sheet undergoing a first-order chemical reaction is investigated. The rheological behaviour of the elastico-viscous fluid is characterised through Walters' liquid model (B′ formulation). By invoking similarity transformations, the controlling partial differential equations are recast into a coupled system of nonlinear self-similar ordinary differential equations subject to pertinent boundary constraints. These nonlinear relations are subsequently reduced to a set of first-order differential equations accompanied by their associated boundary specifications. The resulting system is tackled numerically via MATLAB's intrinsic boundary-value solver bvp4c. The numerical solutions thus obtained are employed to construct velocity and concentration distributions for varying magnitudes of the governing parameters. Critical examination of the generated profiles demonstrates that both the hydrodynamic field and mass transport phenomena are profoundly modulated by the influence of the controlling flow parameters.

## Manuscript Information

- **ISSN No:** 2583-7397
- **Received:** 08-09-2025
- **Accepted:** 30-10-2025
- **Published:** 05-11-2025
- **IJCRM:**4(6); 2025: 11-18

- **Plagiarism Checked:** Yes
- **Peer Review Process:** Yes

## How to Cite this Article

Saha. B. K. Transient Boundary-Layer Dynamics of An Elastico-Viscous Medium Across a Deformable Sheet Subjected to Chemical Reactivity. Int J Contemp Res Multidiscip. 2025;4(6):11-18.

**Access this Article Online**

www.multiarticlesjournal.com

**KEYWORDS:** Unsteady Flow; Elastico-Viscous Fluid; Boundary Layer; Deforming Surface; Chemical Reaction.

## 1. INTRODUCTION

The power-law model is commonly applied to describe fluids whose viscosity varies with shear rate. However, it fails to account for elastic effects. In contrast, second and third-grade fluid models can capture elasticity, but their viscosity does not depend on shear rate (Hayat *et al*. [1]. Additionally, these models cannot represent stress relaxation phenomena. Furthermore, these models fail to capture stress relaxation effects. Conversely, the Maxwell constitutive framework**,** classified within the family of rate-type viscoelastic fluids, possesses the inherent capability to capture stress-relaxation phenomena**,** thereby securing broader recognition and applicability (Abel *et al.* [2]). Unlike formulations involving shear-dependent viscosity, this model circumvents such analytical intricacies in boundary-layer investigations, thereby enabling the analysis with particular emphasis on the role of fluid elasticity in governing boundary-layer dynamics (Heyhat and Khabazi [3]).

The burgeoning interest in magneto-hydrodynamic (MHD) phenomena is principally attributed to its extensive spectrum of practical applications, encompassing domains such as petroleum and natural gas extraction, geophysical fluid dynamics, and innovations in agro-engineering systems**.** The modulation of electrically conducting fluids by applied magnetics flux exerts a decisive influence on the operational efficiency of diverse industrial devices, including hydrodynamic bearings, MHD-based generators, and electromagnetic pumps**.** Beyond the industrial realm, MHD has demonstrated versatility within biomedical engineering, where it underpins techniques for tumour ablation, acceleration of wound healing, gastric therapies, and sterilisation of surgical instruments (Shehzad and Heyhat [4–5]). Investigations of MHD boundary-layer dynamics under thermal stratification have elucidated that intensification of the magnetic interaction parameter suppresses the velocity field, while simultaneously inducing a transient intensification of the skin-friction coefficient. Analogous observations were reported by Tian et al. [6], who analysed the coupled effects of radiative optical characteristics and Lorentz body forces on MHD boundary-layer flow past a deformable surface. Complementary studies have also broadened the scope of inquiry: one examined the existence of dual similarity solutions in the context of MHD transport over a nonlinear porous shrinking sheet immersed in a viscous medium, whereas another, conducted by Jusoh *et al.* [7], explored MHD-driven rotating boundary layers in the presence of a permeable stretching/shrinking sheet.

The analysis of fluid flow and thermal transport attains heightened complexity when examined within porous domains exhibiting spatially varying permeability. In such systems, the flow behaviour and thermal transport characteristics are significantly influenced by spatial variations in permeability (Ullah *et al.* [8]). The heterogeneous structure of the porous material creates intricate interactions between the fluid and the matrix, leading to fluctuations in velocity, pressure, and temperature. These variations can reduce the efficiency of heat transfer and may trigger flow instabilities, including vortex formation and flow recirculation zones (Santos-Moreno *et al.* [9]). Within porous structures, both convection and conduction contribute to heat transfer, while changes in porosity introduce thermal non-uniformity. Consequently, the thermal field within a porous substrate undergoes modulation as the fluid traverses' zones of spatially heterogeneous permeability (Ullah [10]). The development of robust predictive frameworks and high-fidelity models for a wide spectrum of engineering and environmental applications—ranging from subsurface hydrological processes to renewable energy systems—necessitates an interdisciplinary synthesis of fluid dynamics, heat-transfer theory, and porous-media physics. This requirement originates from the highly nonlinear interaction between fluid momentum transfer and heat transport processes embedded in spatially heterogeneous porous frameworks, a topic that has recently attracted considerable research attention across multiple dimensions (Sowmiya and Kumar, Nabwey *et al.*, Reddy *et al.*, Rehman and Salleh [11–14]).

Moreover, hybrid nanofluids—engineered through the suspension of multiple distinct nanoparticle species within a base carrier fluid—have been employed to augment the thermo-physical performance beyond that achievable with conventional mono-nanoparticle formulations, as the combined physical characteristics of different nanoparticles promote enhanced energy transfer (Gangadhar *et al.* [15]). Magnetically influenced, yield-stress-based hybrid nanofluid (with sodium alginate as a carrier) behaves when subjected to squeezing forces, while also considering the coupled thermal and mass diffusion effects (Soret and Dufour) by Noor *et al*. [16].

Several researchers ([17–18]) have investigated unsteady stretching surface problems under various conditions, employing similarity transformations to reduce the governing unsteady boundary-layer model is mapped into a system of ordinary differential equations. Mukhopadhyay and Bhattacharyya [19] conducted an assessment of the transient flow dynamics of Maxwell fluid along a stretching surface subjected to a chemical reaction.

## 2. Governing Equations and Formulation:

A bidirectional laminar boundary-layer transport accompanied by mass transport of an incompressible non-Newtonian fluid over an unsteady stretching sheet is explored. The solute concentrations prescribed at the sheet and in the far-field are represented by $C_W$ and $C_\infty$, respectively. The diffusing species is assumed to participate in a first-order homogeneous chemical reaction governed by a time-dependent rate constant. $Z_1$.

For t $<$ 0Both fluid and mass flows are persistent, while unsteadiness arises at t = 0. The sheet issues from a slit at the origin (x = 0, y = 0) and stretches with a velocity U(x,t) = $\frac{bx}{1-\alpha t}$ where b and $\alpha$ are positive constants of dimension $(time)^{-1}$.

In this formulation, the parameter $b$ characterises the primary stretching rate, whereas the term $\frac{b}{1-\alpha t}$ signifies the instantaneous effective stretching rate, which progressively amplifies as time advances. Within the framework of polymer extrusion, the temporal evolution induces variations in the

physico-mechanical attributes of the emerging sheet. The corresponding system of governing equations is expressed as follows:

$$\frac{\partial u}{\partial x}+\frac{\partial v}{\partial y}=0 \tag{2.1}$$

$$\frac{\partial u}{\partial t}+u\frac{\partial u}{\partial x}+v\frac{\partial u}{\partial y}=v\frac{\partial^2 u}{\partial y^2}-\frac{k_0}{\rho}\left[\frac{\partial}{\partial t}\left(\frac{\partial^2 u}{\partial y^2}\right)+u\frac{\partial^3 u}{\partial x\partial y^2}+v\frac{\partial^3 y}{\partial y^3}-\frac{\partial u}{\partial y}\frac{\partial^2 u}{\partial x\partial y}-\frac{\partial v}{\partial y}\frac{\partial^2 u}{\partial y^2}\right] \tag{2.2}$$

$$\frac{\partial c}{\partial t}+u\frac{\partial c}{\partial x}+v\frac{\partial c}{\partial y}=D\frac{\partial^2 c}{\partial y^2}-z_1(c-c_\infty) \tag{2.3}$$

**Fig. 1 .1.** Geometric Configuration of the Flow Field

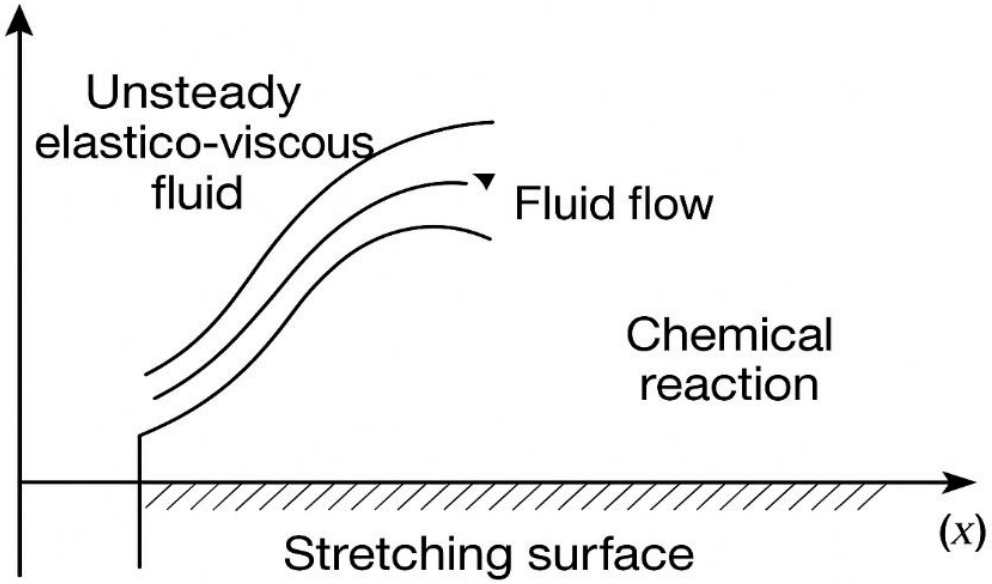


In this context, u and v correspond to the respective velocity components aligned with the Cartesian axes; x and y designate the kinematic viscosity of the working fluid; c signifies the scalar field describing species concentration within the medium; D denotes the molecular diffusivity of the solute dispersed in the fluid. The reaction kinetics, expressed as a function of temporal variation, are given by $z_1(t)=\frac{z_0}{1-\alpha t}$ where $z_0$ It is a constant. A positive value of $z_1>0$ corresponds to a destructive reaction, while a negative value $z_1<0$ Indicates a constructive reaction.

The formulation of the problem adheres to the subsequent set of boundary constraints:

$$u=U(x,t), v=0, \qquad c=c_w(x,t)\ at\ y=0 \tag{2.4}$$

$$u\to 0, \qquad c\to\infty\ as\ y\to\infty \tag{2.5}$$

The sheet's surface concentration varies with both position and time, defined as $c_w(x,t)=c_\infty+bx(1-\alpha t)^{-2}$, where $c_\infty$ Is the uniform free-stream concentration. For ($b>0$) $c_w$ increases with x; for ( $b<0$ ), it decreases, with the variation amplifying over time. The relations for $U(x,t)$, $c_w(x,t)$ and $z_1(t)$ are valid for $\alpha^{-1}$.

We define u and v through the following expressions:

$$u=\frac{\partial\psi}{\partial y}, v=-\frac{\partial\psi}{\partial x}\ and\ \phi=\frac{c-c_\infty}{c_w-c_\infty} \tag{2.6}$$

Similarity-based transformation

$$\eta = y\sqrt{\frac{b}{\upsilon(1-\alpha t)}}, \qquad \psi = \sqrt{\frac{\upsilon b}{1-\alpha t}}xf(\eta), \qquad c = c_\infty + bx(1-\alpha t)^{-2}\phi(\eta) \tag{2.7}$$

By applying relations (2.6) and (2.7) to equations (2.2) and (2.3), the governing equation reduces to

$$M\left(\frac{\eta}{2}f'' + f'\right) + (f')^2 - ff'' - f''' + k_1[\,M\frac{\eta}{2}f'^v + (2M+1)f''' + ff'^v + f'f''' - (f'')^2 = 0 \tag{2.8}$$

$$M\left(\frac{\eta}{2}\phi' + 2\phi\right) + f'\phi - f\phi' - \frac{1}{Sc}\phi'' - \gamma\phi = 0 \tag{2.9}$$

Here, M = $\frac{\alpha}{b}$ Denotes the unsteadiness parameter, $k_1 = \frac{k_0 b}{\mu(1-\alpha t)}$ represents the elastico-viscous parameter, Sc = $\frac{\upsilon}{D}$ Is the Schmidt number, and $\gamma = \frac{z_0}{b}$ corresponds to the reaction rate parameter

Under the transformation, the boundary conditions become

$$f'(\eta) = 1, f(\eta) = 0, \phi(\eta) = 1 \quad at\ \eta = 0 \tag{2.10}$$
$$f'(\eta) \to 0, \qquad \phi(\eta) \to 0 \ as\ \eta \to \infty \tag{2.11}$$

## 3. Solution Scheme

Equations (2.8) and (2.9), representing the self-similar nonlinear form, are transformed into first-order differential relations specified by:

$$f = z_1, f' = z_2,\ f'' = z_3, f''' = z_4\ , \phi = z_5, \phi' = z_6 \tag{3.1}$$

From relation (3.1), it follows that.

$$z_1' = z_2, z_2' = z_3, z_3' = z_4, z_5' = z_6 \tag{3.2}$$

Employing relations (3.1) and (3.2), equations (2.8) and (2.9) may be expressed as:

$$z_4' = \frac{1}{M\frac{\eta}{2} + z_1}\left[z_3^2 - z_2 z_4 - (2M+1)z_4 + \frac{1}{k_1}\left\{z_1 z_3 + z_4 - z_2^2 - M\left(\frac{\eta}{2}z_3 + z_2\right)\right\}\right] \tag{3.3}$$

$$z_6' = sc\,\{\,z_2 z_5 - z_1 z_6 - \gamma z_5 + M\left(\frac{\eta}{2}z_6 + 2z_5\right) \tag{3.4}$$

While the boundary conditions (2.10) and (2.11) are transformed as follows:

$$z_1(0) = 0, z_2(0) = 1\ and\ \ z_3(0) = 0\ , z_5(0) = 1 \tag{3.5}$$
$$z_2(\infty) = 0, z_5(\infty) = 0 \tag{3.6}$$

Equations (3.3) – (3.4), subject to boundary constraints (3.5) – (3.6), are numerically resolved via MATLAB's **bvp4c** scheme for a range of flow-parameter values examined in this study.

## 4. Results and Discussion:

The MATLAB solver **bvp4c** is used to compute velocity and concentration profiles, demonstrating the effect of governing parameters on flow behaviour (Figures 2–8). Validation is carried out by comparing the computed skin friction coefficient $f''(0)$ With established results showing close agreement (Table 4.1) and confirming accuracy.

**Table 4.1:** The values of $f''(0)$ corresponding to different unsteadiness parameters M when $k_1$=0

| M | Sharidan *et al.* [17] | Chamakha *et. al.* [18] | Mukhopadhyay and Bhattacharyya [19] | Present Study |
|---|---|---|---|---|
| 0.8 | -1.261042 | -1.261512 | -1.261479 | -1.261450 |
| 1.2 | -1.377722 | -1.378052 | -1.377850 | -1.377845 |

Fig.4.1. The velocity distribution corresponding to different values of the elastico-viscous coefficient $k_1$ Are presented. The velocity exhibits an initial attenuation, followed by a progressive augmentation with increasing elastico-viscous effects, and ultimately undergoes a downstream decay for a prescribed unsteadiness parameter M.

Fig.4.2. Depicts the implication of the unsteadiness parameter M on the velocity distribution. $f'(\eta)$. With increasing M, the

velocity along the sheet exhibits a marked reduction, while farther from the surface, it reveals non-uniform fluctuations. In the initial region, the momentum diffusion-layer thickness, both adjacent to and away from the sheet, enlarges with higher M. The special case M = 0 signifies the steady-state regime.

Fig.4.3 presents the concentration distribution. $\emptyset(\eta)$ Under varying magnitudes of the unsteadiness parameter M. The findings reveal that concentration exhibits an initial rise, followed by a gradual decay as M increases. The mass transfer rate, though significant near the onset, diminishes progressively with higher M. Moreover, at any fixed spatial location, concentration declines sharply with increasing M. Since fluid motion is induced exclusively by the stretching sheet—where surface concentration exceeds the ambient free-stream level—the concentration profile consistently decreases with $\eta$ Under the influence of the elastico-viscous parameter.

Fig.4.4. Depicts the implication of the Schmidt number *Sc* on the concentration distribution. $\emptyset(\eta)$. An intriguing behaviour emerges wherein concentration first exhibits a rise but subsequently diminishes with escalating *Sc*. Furthermore, the solute diffusion-layer thickness contracts as *Sc* grows and ultimately approaches a stabilised state at a finite location.

Fig.4.5. Depicts the consequence of the generative reaction coefficient. $\gamma$ (< 0) on the concentration distribution $\emptyset(\eta)$. With increasing $\gamma$ The concentration diminishes significantly, resulting in a lowered mass diffusion rate. For constructive chemical reactions $\gamma$ (< 0), the concentration field undergoes a marked reduction under the governing influence of the elastico-viscous effects. The profile first decreases, then rises after a certain distance as the reaction rate parameter decreases, and eventually stabilises at a point along the sheet. Additionally, the diffusion layer thickness is found to decrease progressively.

Fig.4.6. Portrays the influence of the destructive reaction coefficient. $\gamma$ (> 0) on the concentration distribution $\emptyset(\eta)$. The concentration exhibits a pronounced decline with increasing. $\gamma$, yet beyond $\eta$=2 it rises, thereby augmenting the mass diffusion rate from the fluid domain toward the surface. Owing to the elastico-viscous parameter, concentration initially drops rapidly, then decreases more gradually with rising reaction rate parameter, and eventually stabilises at the sheet. The diffusion layer thickness initially grows quickly due to the combined elastic and viscous effects, but with further increase in the reaction rate parameter, it gradually becomes thinner.

Fig.4.7. As the elastico-viscous parameter escalates, the concentration profile $\emptyset(\boldsymbol{\eta})$ drops sharply at $\eta$=4, then rises quickly and converges at a certain point. This trend indicates that higher elastico-viscous parameter values cause a significant reduction in the mass diffusion rate. In general, the concentration distribution diminishes with rising elastico-viscous parameter, whereas the thickness of the diffusion layer correspondingly expands.

**Fig. 4.1.** Implication of $k_1$ on Velocity Profile $f'(\eta)$

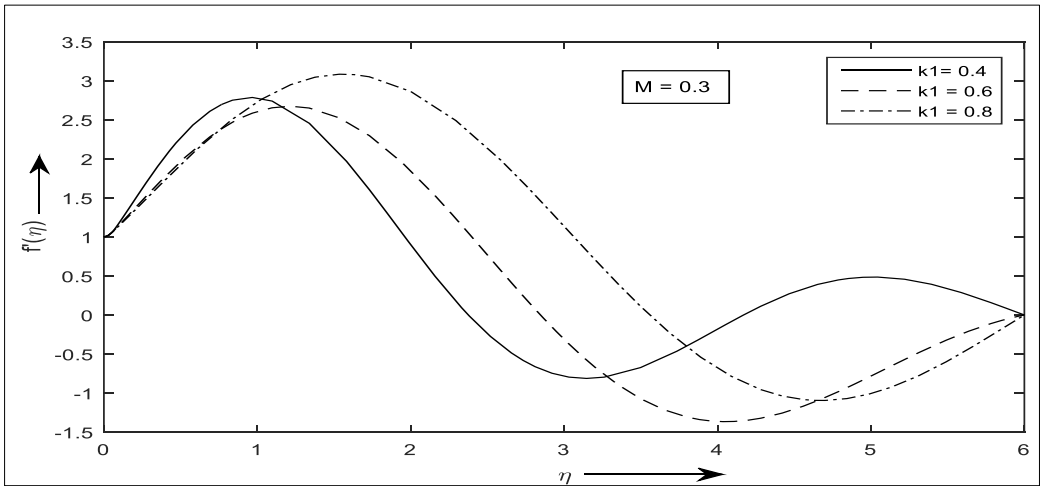

**Fig.4.2.** Implication of M on Velocity Profile $f'(\eta)$

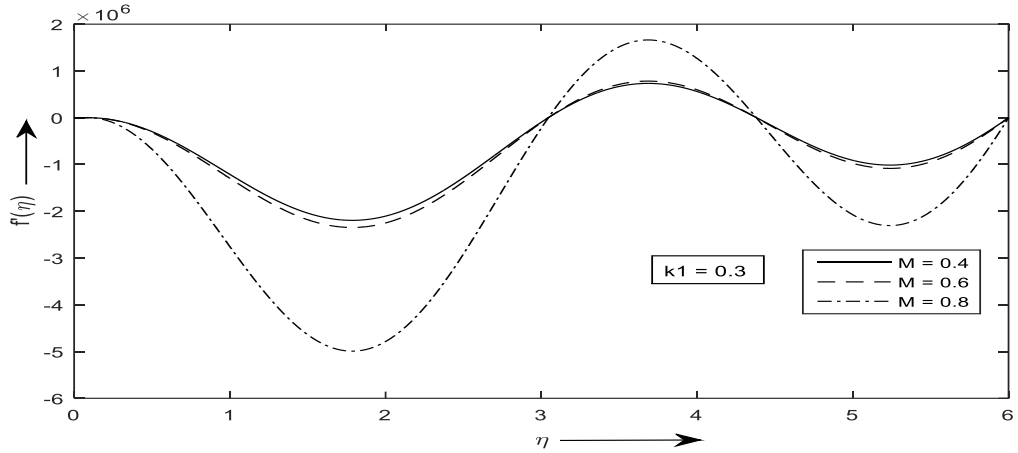


**Fig.4.3.** Implication of M on Concentration Profile $\emptyset(\eta)$

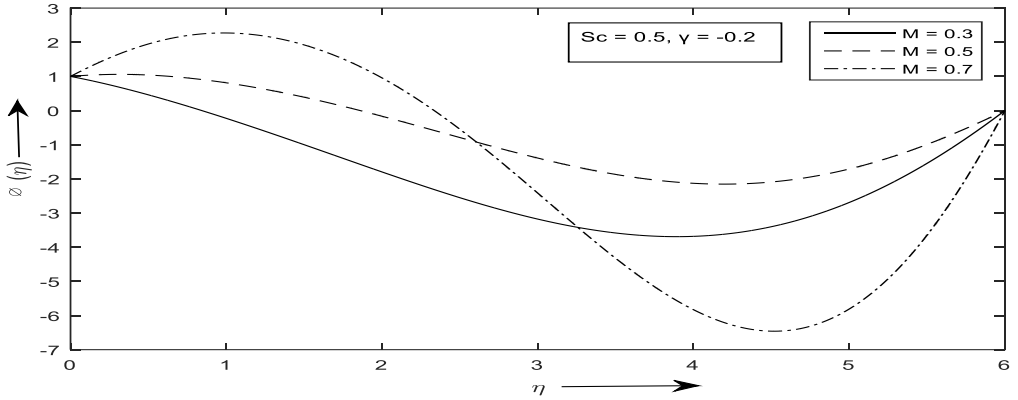


**Fig.4.4.** Implication of Sc on Concentration Profile $\emptyset(\eta)$

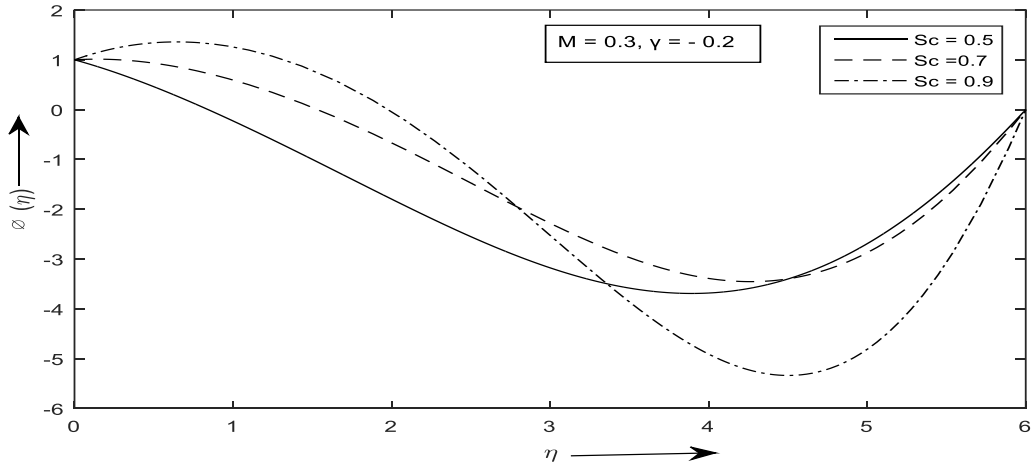

**Fig4.5.** Implication of $\gamma$ ($\gamma < 0$) on Concentration Profile $\emptyset(\eta)$

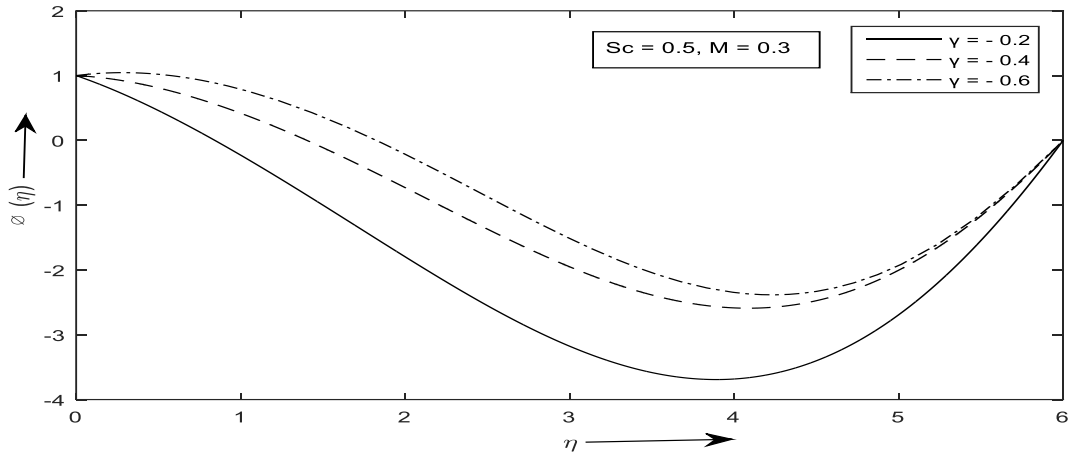


**Fig.4.6.** Implication of $\gamma$ ($\gamma > 0$) on Concentration Profile $\emptyset(\eta)$

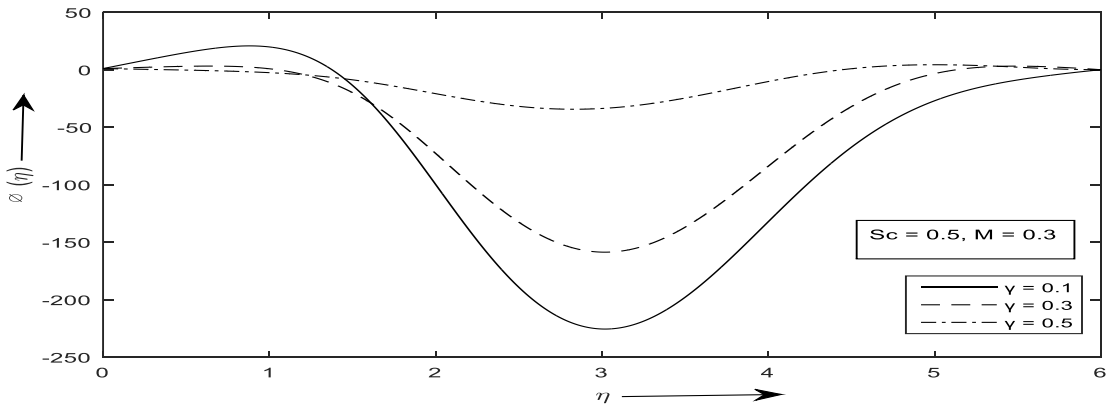


**Fig.4.7.** Implication of $k_1$ On Concentration Profile $\emptyset(\eta)$

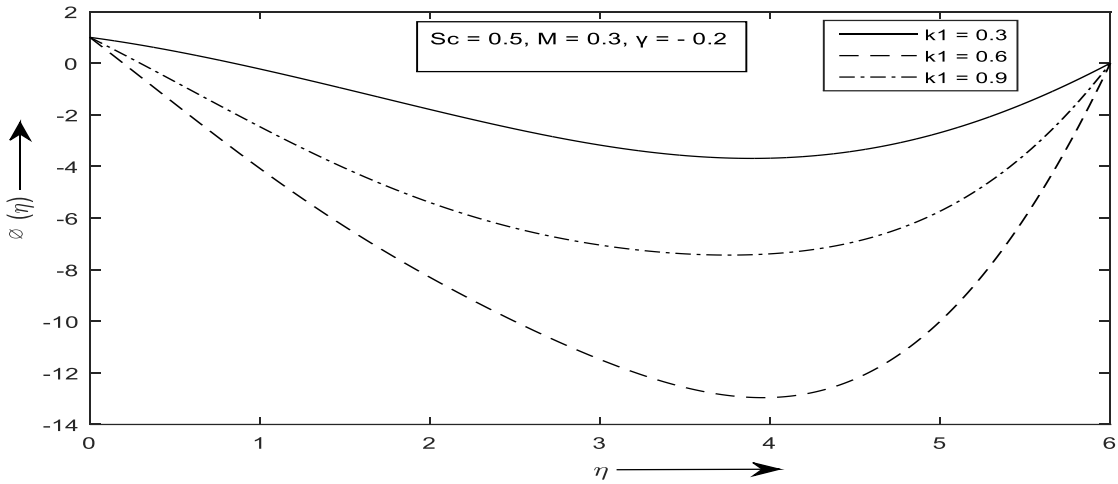

## CONCLUSION

The key findings of this research are summarised below:

(i) The velocity profile climbs down and oscillates for the growth of the elastic-viscous parameter, and oscillates after traversing a few distances on the sheet with the growth of the unsteadiness parameter.

(ii) The concentration profile decreases with the growth of the fluid flow parameter involved in this research.

(iii) The sheet surface experiences a decrease in mass transfer rate as growth of both unsteadiness and elastico-viscous parameter.

## REFERENCES


1. Hayat T, Shehzad SA, Qasim M, Obaidat S. Steady flow of Maxwell fluid with convective boundary conditions. *Z Naturforsch A.* 2011;66(4–5):417–422.
2. Abel MS, Tawade JV, Nandeppanavar MM. MHD flow and heat transfer for the upper-convected Maxwell fluid over a stretching sheet. *Meccanica.* 2011. doi:10.1007/s11012-011-9448-7.
3. Heyhat MM, Khabazi N. Non-isothermal flow of Maxwell fluids above fixed flat plates under the influence of a transverse magnetic field. *Proc IMechE Part C J Mech Eng Sci.* 2010;225(10). doi:10.1243/09544062JMES224.
4. Shehzad SA, Abdullah Z, Alsaedi A, Abbasi FM, Hayat T. Thermally radiative three-dimensional flow of Jeffrey nanofluid with internal heat generation and magnetic field. *J Magn Magn Mater.* 2016; 397: 108–114.
5. Hayat T, Waqas M, Khan MI, Alsaedi A. Impacts of constructive and destructive chemical reactions in magnetohydrodynamic (MHD) flow of Jeffrey liquid due to nonlinear radially stretched surface. *J Mol Liq.* 2017; 225:302–310.
6. Tian X, Li B, Zhang J. The effects of radiation optical properties on the unsteady 2D boundary layer MHD flow and heat transfer over a stretching plate. *Int J Heat Mass Transf.* 2017; 105: 109–112.
7. Jusoh R, Nazar R, Pop I. Magnetohydrodynamic rotating flow and heat transfer of ferrofluid due to an exponentially permeable stretching/shrinking sheet. *J Magn Magn Mater.* 2018; 465: 365–374.
8. Ullah I, Alam MM, Rahman MM, et al. Theoretical analysis of entropy production in exothermic/endothermic reactive magnetised nanofluid flow through curved porous space with variable permeability and porosity. *Int Commun Heat Mass Transf.* 2022; 139:106390.
9. Santos-Moreno M, Valencia-Negrete CV, Fernandez-Anaya G. Conformable derivatives in viscous flow describing fluid through porous medium with variable permeability. *Fractals.* 2022;30(9):2250178.
10. Ullah I. Activation energy with exothermic/endothermic reaction and Coriolis force effects on magnetised nanomaterials flow through Darcy–Forchheimer porous space with variable features. *Waves Random Complex Media.* 2022;35(1):398–411. doi:10.1080/17455030.2021.2023779.
11. Sowmiya C, Kumar BR. MHD Maxwell nanofluid flow over a stretching cylinder in porous media with microorganisms and activation energy. *J Magn Magn Mater.* 2023; 582:171032.
12. Nabwey HA, El-hakiem A, Khan WA, et al. Magnetic Williamson hybrid nanofluid flow around an inclined stretching cylinder with Joule heating in a porous medium. *Chem Eng J Adv.* 2024; 18: 100604.
13. Reddy YD, Goud BS, Nisar KS, et al. Heat absorption/generation effect on MHD heat transfer fluid flow along a stretching cylinder with a porous medium. *Alexandria Eng J.* 2023;64: 659–666.
14. Rehman A, Salleh Z. Influence of Marangoni convection on magnetohydrodynamic viscous dissipation and heat transfer on hybrid nanofluids in a rotating system between two surfaces. *Mathematics.* 2021;9(18):2242.
15. Gangadhar K, Rani MS, Wakif A. Improved slip mechanism and convective heat impact for ternary nanofluidic flowing past a Riga surface. *Int J Mod Phys B.* 2024.
16. Noor NAM, Mahadi S, Nordin NS, Arbin N, Shafie S, Admon MA, Lim YJ. Squeezing MHD flow of sodium alginate-based Casson hybrid nanofluid with Soret and Dufour effects. *J Adv Res Fluid Mech Therm Sci.* 2024;116(1):97–115.
17. Sharidan S, Mahmood T, Pop I. Similarity solutions for the unsteady boundary layer flow and heat transfer due to a stretching sheet. *Int J Appl Mech Eng.* 2006; 11:647–654.
18. Chamkha AJ, Aly AM, Mansour MA. Similarity solution for unsteady heat and mass transfer from a stretching surface embedded in a porous medium with suction/injection and chemical reaction effects. *Chem Eng Commun.* 2010;197: 846–858.
19. Mukhopadhyay S, Bhattacharyya K. Unsteady flow of a Maxwell fluid over a stretching surface in the presence of chemical reaction. *J Egypt Math Soc.* 2012;20(3):229–34.




**About the Corresponding Author**

**Dr. Bikash Koli Saha** is an Independent Researcher and Educator in Mathematics, specialising in fluid dynamics, boundary layer theory, and mathematical physics. Formerly an Assistant Professor at Don Bosco College, Tura, he remains dedicated to advancing research in fluid mechanics, heat transfer, and applied differential equations through analytical precision and innovation.